2013-05-26

A Novel Class of Polymeric pH-Responsive MRI CEST Agents

UTD AUTHOR(S): Shanrong Zhang, Masaya Takahashi, A Dean Sherry and Jinming Gao

ChemComm

RSC Publishing

COMMUNICATION

View Article Online
View Journal | View Issue

A novel class of polymeric pH-responsive MRI CEST agents†

Cite this: *Chem. Commun.*, 2013, **49**, 6418

Received 4th April 2013,
Accepted 26th May 2013

DOI: 10.1039/c3cc42452a

www.rsc.org/chemcomm

Shanrong Zhang,[ab] Kejin Zhou,[a] Gang Huang,[a] Masaya Takahashi,[b] A. Dean Sherry*[bc] and Jinming Gao*[ac]

In this communication, we report that ionizable, tertiary amine-based *block* copolymers can be used as pH-responsive contrast agents for magnetic resonance imaging (MRI) through the chemical exchange saturation transfer (CEST) mechanism. The CEST signal is essentially "off" when the polymers form micelles near physiological pH but is activated to the "on" state when the micelles dissociate in an acidic environment.

Balaban and coworkers first reported a new class of contrast agents for magnetic resonance imaging (MRI) based on a chemical exchange saturation transfer (CEST) mechanism.[1,2] In biological systems, many endogenous CEST agents exist either as small biomolecules or macromolecules with exchangeable –NH or –OH protons.[3–6] Exogenous CEST agents can also be designed to respond to a variety of physiological signals such as pH, temperature, enzyme activity or metabolite levels.[7–13] This new technology offers a multitude of new venues for *in vivo* molecular imaging using standard MRI scanners.

In our previous studies, we have reported a series of tertiary amine-based *block* copolymers, such as poly(ethylene glycol)-*b*-poly[2-(diisopropylamino)ethyl methacrylate] (PEG-*b*-PDPA), that form micelles at pH 7.4 and dissociate over a sharp pH range below 6.3. The micelles dissociate into unimers in acidic environments due to the switch of the amine *block* of PDPA from the hydrophobic to the hydrophilic/charged state that parallels protonation of tertiary amine groups (Scheme 1).[14,15] The pH response is sharp (ΔpH $<$ 0.25 pH units) and tunable (the transition pH, pH_t, is adjustable by changing the side chains of tertiary amines). Since the major difference between the micelle and unimer states is the protonation of tertiary amines (where the resulting ammonium groups have exchangeable protons), we anticipated that these copolymers may also serve as activatable MRI contrast agents *via* a CEST mechanism. Conceivably, the CEST signal would be silent near physiological pH (*i.e.* the micellar form does not contain exchangeable protons) but would be turned "on" in acidic environments after the micelles dissociate into protonated unimers having exchangeable protons.

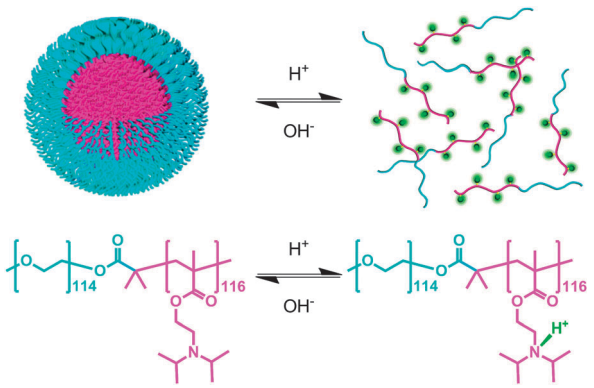

Scheme 1 The micelle–unimer equilibrium in the *block* copolymer, PEG_{114}-*b*-$PDPA_{116}$, is exquisitely sensitive to pH.

To investigate the feasibility of this approach, a PEG_{114}-*b*-$PDPA_{116}$ copolymer (114 and 116 refer to the numbers of repeating units in PEG and PDPA segments, respectively) was synthesized and used as a model system (Scheme 1 and Fig. S1 in the ESI†). Two major aspects were considered: (1) PEG-*b*-PDPA copolymers had been intensively characterized in previous studies as ultra pH-responsive fluorescent probes;[15] and (2) the pK_a of PEG-*b*-PDPA is *ca.* one pH unit below the physiological pH so that it will have large enough differences to be silent in blood yet potentially shows a CEST signal only from acidic tissues. Experimentally, the pK_a of PEG_{114}-*b*-$PDPA_{116}$ as determined by pH titration (Fig. S2 in the ESI†) was 6.27. This pK_a is 0.4 pH unit lower than that reported for a similar copolymer with a shorter $PDPA_n$ segment (n = 80) and additional

[a] *Department of Pharmacology, Harold C. Simmons Comprehensive Cancer Center, University of Texas Southwestern Medical Center, Dallas, Texas 75390, USA. E-mail: jinming.gao@utsouthwestern.edu*

[b] *Advanced Imaging Research Center, University of Texas Southwestern Medical Center, Dallas, Texas 75390, USA. E-mail: dean.sherry@utsouthwestern.edu*

[c] *Department of Chemistry, University of Texas at Dallas, Richardson, Texas 75083, USA*

† Electronic supplementary information (ESI) available: Polymer synthesis, micelle preparation, pH titration, CMC additional DLS and NMR data. See DOI: 10.1039/c3cc42452a

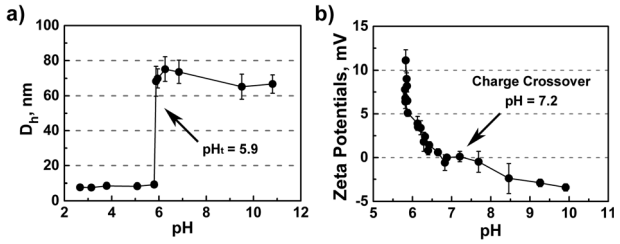

Fig. 1 (a) The hydrodynamic diameter (D_h, nm) and (b) zeta potential (mV) of PEG-*b*-PDPA as a function of pH.

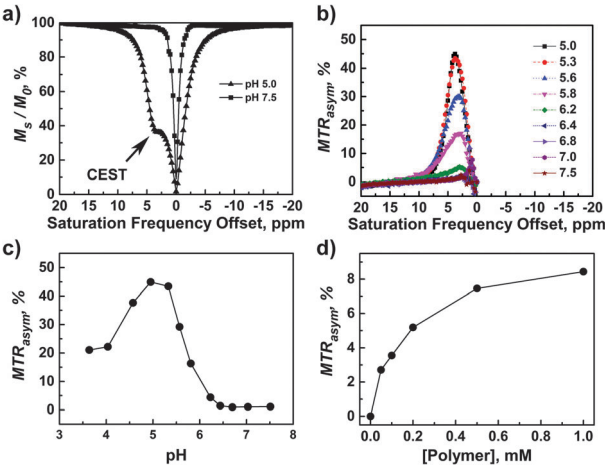

Fig. 2 (a) Representative CEST spectra of PEG-*b*-PDPA at pH 5.0 and 7.5, respectively; (b) a plot of MTR$_{asym}$ *versus* the saturation frequency offset at the pH range between 5.0 and 7.5; (c) a plot of MTR$_{asym}$ (±3.8 ppm) *versus* pH and (d) a plot of MTR$_{asym}$ *versus* PEG-*b*-PDPA copolymer concentration at a fixed pH of 5.8. All data were acquired on a B_0 = 9.4 T NMR spectrometer (400 MHz for ^{1}H).

fluorescent dyes (tetramethyl rhodamine).[15] In addition, the critical micelle concentration (CMC) (Fig. S3, ESI†) was found to be 0.15 μg ml^{-1} for PEG$_{114}$-*b*-PDPA$_{116}$, about 6-fold lower than that of PEG$_{114}$-*b*-PDPA$_{80}$ (CMC = 0.9 μg ml^{-1}).[15]

Fig. 1a shows the pH dependence of the hydrodynamic diameter (D_h, nm) of PEG-*b*-PDPA as measured by the dynamic light scattering (DLS). Clearly, the micelle transition occurs at a pH$_t$ of *ca.* 5.9, about 0.4 pH units lower than that of a similar *block* copolymer with a shorter PDPA$_n$ segment (n = 80).[15] To evaluate the protonation status, the zeta potential of PEG-*b*-PDPA was also measured as a function of pH (Fig. 1b). At high pH values where the amines are de-protonated and micelles dominate, the small negative zeta potential reflects small amounts of OH^- and Cl^- anions introduced during sample preparation. As the pH is lowered, protonation (H^+) of the tertiary amines occurs and the PDPA segments acquire positive charge. It is worth noting that the charge crossover point (the point of zero charge) is approximately at pH 7.2, about one pH unit above the pK_a of the amine. In contrast, the zeta potential increases much more dramatically as the pH approaches the pH$_t$ at ~5.9. This indicates that the protonation of the *block* copolymer is dramatically increased during the transition from micelles to unimers.

To examine the CEST feasibility of PEG-*b*-PDPA, the polymer was prepared into micelles at a polymer concentration of 0.5 mM following the published procedures.[14] The stock solution was dispersed in a 0.1 M buffer consisting of 2-(*N*-morpholino)ethanesulfonic acid (MES) and/or 3-morpholinopropane-1-sulfonic acid (MOPS) to achieve a stable pH value. The sample was ultracentrifuged using centrifuge filtration tubes with a 3 kD molecular weight cutoff (MWCO) filter. Samples of buffer alone were tested and found to have no CEST signal (Fig. S4 in the ESI†). Fig. 2a illustrates typical CEST spectra of PEG-*b*-PDPA solution at pH 5.0 and 7.5, respectively. Each data point in a CEST spectrum reflects the intensity of the solvent water signal in the ^{1}H NMR spectrum after applying a 5 s RF saturation pulse at a power level of 9.4 μT at 160 different saturation frequency offsets over the range ±20 ppm.[1,2] The negative peak at 0 ppm in these spectra reflects direct saturation of the solvent water resonance (Note: the chemical shift of bulk water was manually set to 0 ppm to better visualize the CEST peak). At pH 7.5, there is no evidence for the exchanging species that could produce CEST. At pH 5.0, however, the CEST spectrum shows quite a different lineshape, namely, an additional exchange peak appears as a shoulder at *ca.* 2–5 ppm downfield of water. This can be assigned to CEST from the exchangeable protons on the tertiary ammonium groups. Assuming that all protonated tertiary amines have an identical proton exchange rate and chemical shift, this CEST spectrum should fit well to a simple 2-pool chemical exchange model involving proton exchange between R_3N–H^+ and H_2O protons. The solid line in Fig. 2a shows the fit of the CEST data at pH 5.0 to the Bloch equations for a 2-pool model.[16] The ammonium proton lifetime (τ_{ex}) in PEG-*b*-PDPA at pH 5.0 was estimated to be ~890 μs using this fitting procedure. In addition, the corresponding monomeric analogs, *N*,*N*-diisopropylethylamine and *N*,*N*-diisopropylaminoethanol, were found to have similar CEST features (Fig. S5, ESI†). These data support the assignment of the CEST peak appearing near 2–5 ppm to the exchangeable amine proton in the polymeric form of PEG-*b*-PDPA.

The CEST effect can be better visualized in a plot of the asymmetric intensity difference between the MRI signal with presaturation at the frequency of exchanging protons (on-freq) and the MRI signal with presaturation at an equivalent frequency on the opposite side of water (off-freq),[13] *i.e.*, $MTR_{asym} = [(M_s/M_0)_{on\ freq} - (M_s/M_0)_{off\ freq}]$, as shown in Fig. 2b. For clarity, only those MTR$_{asym}$ spectra over the pH range 5.0 to 7.5 were shown. All CEST spectra and the corresponding MTR$_{asym}$ spectra are shown in Fig. S6 (ESI†). For PEG-*b*-PDPA, the exchanging protons are activated over a rather broad range of pH values, reaching a maximum at pH ~5. Shown in Fig. 2c is a plot of MTR$_{asym}$ *vs.* pH for this system. There are three distinct phases in this plot: (1) the 1st phase above pH 6.5 corresponds to the non-protonated micelle state where CEST is "off"; (2) the 2nd phase between pH 5 and 6.5 shows a variable CEST "on" region where the sample is partially converted from micelles to unimers and begins to protonate; and (3) the 3rd phase below pH ~5 where proton exchange gradually becomes too slow to meet the exchange requirement for CEST. Such a bell-shaped dependence of CEST *versus* pH values was previously observed in a paramagnetic CEST system.[17] In the 1st and 2nd phases, the CEST effects present a typical switch from the totally "off"

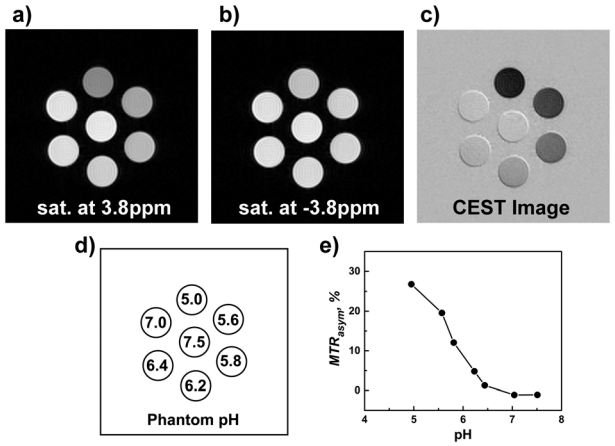

Fig. 3 9.4 T MRI images (a–c) of a phantom consisting of seven plastic tubes containing 0.5 mM PEG-*b*-PDPA solutions in the presence of 0.1 M MES–MOPS buffers at different pH values (d). The images were obtained sequentially by applying a 3 s pre-saturation pulse at either +3.8 ppm or −3.8 ppm at a power level of 8.2 μT, respectively. The CEST image (c) was obtained by image subtraction. The quantified MTR_{asym} between the images (c) and (b) were plotted in (e), which were further normalized to zero for the background.

(pH > 6.5) to gradually ''on'' (pH < 6.5). By comparing the data shown in Fig. 1b and 2c, one could conclude that the CEST effects should be proportional to the protonation percentages of the tertiary amino groups. These NMR spectroscopic data do reveal the feasibility that PEG-*b*-PDPA might be able to serve as an MRI CEST agent over a physiologically relevant pH range.

The sensitivity of detection of a contrast agent is an important parameter. Shown in Fig. 2d is a plot of MTR_{asym} *vs.* the polymer concentration at pH 5.8 (Note: this data set was acquired using a shorter saturation duration time of 3 s). This shows that an ~0.1 mM polymer is required to produce the ~3% CEST signal. This sensitivity is similar in order of magnitude to other small molecular CEST agents[1,2] or polymeric CEST agents on a per-monomer basis.[18]

To further demonstrate the feasibility of using CEST to image pH by MRI, a phantom was prepared consisting of seven plastic tubes filled with 0.5 mM PEG-*b*-PDPA solutions at different pH values (Fig. 3d). A 3 s saturation pulse (B_1 = 8.2 μT) was applied at the different frequency offsets, varying from +10 ppm to −10 ppm with a decreased step of 0.2 ppm. Shown in Fig. 3a and b are the raw images at saturation frequency offsets of +3.8 ppm and −3.8 ppm, respectively. The CEST image (Fig. 3c) was obtained *via* an image subtraction pixelwise (Fig. 3a and b). Shown in Fig. 3e is a quantified plot of MTR_{asym} (±3.8 ppm) as a function of pH. The trend has a very similar pattern to that of the spectroscopic data shown in Fig. 2c but the absolute values were different because the image intensities are related to many factors such as the MRI hardware settings, the imaging pulse sequences, *etc.*

In summary, we have shown that ionizable polymer-based CEST probes may be used as pH-responsive MRI CEST agents. This system is unique in that CEST is essentially ''off'' at normal physiological pH and only switched ''on'' in an acidic environment. This pH-activatable micelle platform may find useful applications for *in vivo* MRI molecular imaging of acidosis-related metabolic diseases as well as for monitoring the pH-responsive drug delivery using pH-responsive micelles as nanocarriers.

This research was supported by grants from the National Institutes of Health to JG (CA129011 and EB013149) and ADS (CA-115531, EB-004582 and EB-015908).

Notes and references

1 K. M. Ward, A. H. Aletras and R. S. Balaban, *J. Magn. Reson.*, 2000, **143**, 79–87.
2 K. M. Ward and R. S. Balaban, *Magn. Reson. Med.*, 2000, **44**, 799–802.
3 J. Zhou, J. F. Payen, D. A. Wilson, R. J. Traystman and P. C. M. van Zijl, *Nat. Med.*, 2003, **9**, 1085–1090.
4 J. Zhou and P. C. M. van Zijl, *Prog. Nucl. Magn. Reson. Spectrosc.*, 2006, **48**, 109–136.
5 A. A. Gilad, M. T. McMahon, P. Walczak, P. T. Winnard, V. Raman, H. W. M. van Laarhoven, C. M. Skoglund, J. W. M. Bulte and P. C. M. van Zijl, *Nat. Biotechnol.*, 2007, **25**, 217–219.
6 K. Cai, M. Haris, A. Singh, F. Kogan, J. H. Greenberg, H. Hariharan, J. A. Detre and R. Reddy, *Nat. Med.*, 2012, **18**, 302–306.
7 S. Zhang, M. Merritt, D. E. Woessner, R. E. Lenkinski and A. D. Sherry, *Acc. Chem. Res.*, 2003, **36**, 783–790.
8 S. Aime, S. Crich, E. Gianolio, G. Giovenzana, L. Tei and E. Terreno, *Coord. Chem. Rev.*, 2006, **250**, 1562–1579.
9 M. Woods, D. E. Woessner and A. D. Sherry, *Chem. Soc. Rev.*, 2006, **35**, 500–511.
10 S. Aime, D. D. Castelli, S. G. Crich, E. Gianolio and E. Terreno, *Acc. Chem. Res.*, 2009, **42**, 822–831.
11 M. M. Ali, G. Liu, T. Shah, C. A. Flask and M. D. Pagel, *Acc. Chem. Res.*, 2009, **42**, 915–924.
12 L. M. De Leon-Rodriguez, A. J. M. Lubag, C. R. Malloy, G. V. Martinez, R. J. Gillies and A. D. Sherry, *Acc. Chem. Res.*, 2009, **42**, 948–957.
13 P. C. M. van Zijl and N. N. Yadav, *Magn. Reson. Med.*, 2011, **65**, 927–948.
14 K. Zhou, Y. Wang, X. Huang, K. Luby-Phelps, B. D. Sumer and J. Gao, *Angew. Chem., Int. Ed.*, 2011, **50**, 6109–6114.
15 K. Zhou, H. Liu, S. Zhang, X. Huang, Y. Wang, G. Huang, B. D. Sumer and J. Gao, *J. Am. Chem. Soc.*, 2012, **134**, 7803–7811.
16 D. E. Woessner, S. Zhang, M. E. Merritt and A. D. Sherry, *Magn. Reson. Med.*, 2005, **53**, 790–799.
17 S. Zhang and A. D. Sherry, *International Society for Magnetic Resonance in Medicine, 10th Scientific Meeting & Exhibition*, Honolulu, Hawaii, United States, 2002, p. 2590.
18 N. Goffeney, J. W. M. Bulte, J. Duyn, L. H. Bryant and P. C. M. van Zijl, *J. Am. Chem. Soc.*, 2001, **123**, 8628–8629.

SUPPORTING INFORMATION

A Novel Class of Polymeric pH-Responsive MRI CEST Agents

Shanrong Zhang,[a,b] Kejin Zhou,[a] Gang Huang,[a] Masaya Takahashi,[b] A. Dean Sherry*[,b,c] and Jinming Gao*[,a,c]

[a] Department of Pharmacology, Harold C. Simmons Comprehensive Cancer Center, University of Texas Southwestern Medical Center, Dallas, Texas 75390, USA

[b] Advanced Imaging Research Center, University of Texas Southwestern Medical Center, Dallas, Texas 75390, USA

[c] Department of Chemistry, University of Texas at Dallas, Richardson, Texas 75083, USA

* To whom correspondence should be addressed:

dean.sherry@utsouthwestern.edu or jinming.gao@utsouthwestern.edu

Table of Contents

1) Materials

N,N,N',N",N"-Pentamethyldiethylenetriamine (PMDETA) was purchased from Sigma-Aldrich. 2-(Diisopropyl amino) ethyl methacrylate (DPA) was purchased from Polyscience Company. PEG macroinitiator (MeO-PEG_{114}-Br) were prepared according to the procedure in literature.[1] Other solvents and reagents were used as received from either Sigma-Aldrich or Fisher Scientific Inc.

2) Synthesis of PEG-*b*-PDPA block copolymer

The PEG-*b*-PDPA block copolymer was synthesized by the atom transfer radical polymerization (ATRP) method. First, DPA (2.6 g, 120 mmol), PMDETA (25 μL, 0.12 mmol), and MeO-PEG_{114}-Br (500 mg, 0.1 mmol) were charged into a polymerization tube. Then DMF (1 ml) was added to dissolve the monomer and initiator. After three cycles of freeze-pump-thaw to remove oxygen, CuBr (16 mg, 0.11 mmol) was added into the reaction tube under nitrogen atmosphere, and the tube was sealed *in vacuo*. The polymerization was carried out at 50 ^{o}C for 16 hours. After polymerization, the reaction mixture was diluted with 20 ml THF, and passed through an Al_2O_3 column to remove the catalyst. The THF solvent was removed by rotovap. The residue was dialyzed against the distilled water and lyophilized to provide a white powder. The resulting PEG-*b*-PDPA block copolymers were characterized by ^{1}H 500 MHz NMR, gel permeation chromatography (Viscotek GPCmax, PLgel 5 μm MIXED-D columns by Polymer Labs, THF as eluent at 1 ml/min).

3) Preparation of the micelle solutions for CEST evaluation

Micelles were prepared similar to that of the published procedures.[2] First, 100 mg of the copolymer was dissolved in 5 ml DMF and then added into 40 ml distilled water dropwise under sonication. The mixture was diluted with DI water so that DMF percentage was around 1% (V/V). The DMF was removed through ultrafiltration dialysis with (10 kD) membrane for several times. Then the distilled water was added to adjust the polymer concentration to 15 mg/ml as a stock solution. After micelle formation, the nanoparticles were re-dispersed into 0.1 M MES / MOPS at different pH values and characterized using a 400 MHz NMR spectrometer for CEST efficiencies.

4) pH titration

First, PEG_{114}-*b*-$PDPA_{116}$ copolymer (88 mg) was dissolved in 5 ml 0.1 mol/L HCl and diluted to 20 ml with DI water. The pH titration was carried out by adding the titrant (0.1 - 1 ml increments) of 0.02 M NaOH solution under vigorous magnetic stirring. The pH increase in the range of 2 to 10 was monitored as a function of

the total added volume of NaOH (V_{NaOH}). The pH values were measured using a Mettler Toledo pH meter with a microelectrode.

5) CMC measurements

Critical micelle concentration (CMC) value is the threshold polymer concentration at which micelles would form in solution. CMC of PEG_{114}-*b*-$PDPA_{116}$ copolymer was measured in the 0.2 M sodium phosphate buffer at pH 7.4. First, the stock solution (5 mg/ml) was diluted to different concentrations with the same buffer. In each solution, 5 μL pyrene in THF solution (2×10^{-4} M) was added to 2 ml polymer solution to produce the final pyrene concentration at 5×10^{-7} M. The fluorescence spectra were recorded on a Hitachi fluorometer (F-7500 model) with the excitation wavelength of 339 nm and the excitation and emission slits at 10.0 nm and 1.0 nm, respectively. The I_1 and I_3 values were measured as the maximum emission intensity at *ca*. 372 and 382 nm, respectively. I_1/I_3 ratio was plotted as a function of polymer concentration. I_1/I_3 ratio reflects the polarity of the pyrene environment where partition of pyrene in the hydrophobic micelle core leads to decreased I_1/I_3 values.

6) Preparation of samples for DLS and pH measurements

PEG_{114}-*b*-$PDPA_{116}$ (125 mg) was dissolved in 50 ml DI water by adding 2 ml 1M HCl. After fully dissolved, the total volume was adjusted to 100 ml by adding DI water. The initial pH is measured, $pH_{(initial)}$ = 1.4. This solution was titrated by adding the titrant (0.1 – 1 ml incremnets) of 0.02 M NaOH solution under vigorous magnetic stirring. At pH values of interest, the 1.5 ml mixtures were taken and filtrated through 0.45 μm syringe filters. These samples were used to measure the hydrodynamic diameters and Zeta potentials.

7) DLS protocols

Dynamic light scattering (DLS) was measured on a Zetasizer μV model (with He-Ne laser, λ= 632 nm) (Malvern Instruments Ltd, Worcestershire, UK). For hydrodynamic diameter measurement, Zen0040 disposable micro cuvettes were used as the sample cell, with 173^{o} backscatter (NIBS default), number of runs = 5, duration time = 10 s, six measurements per data point, and automatic attenuation. For the Zeta potential measurement, DTS1060C Clear Disposable zeta cell was used as the sample cell, with automatic measurement duration (minimum 30 and maximum 100), automatic attenuation, and six measurements per sample.

8) NMR CEST characterization

^{1}H NMR CEST evaluation was performed with an Agilent Technologies 9.4 T vertical bore NMR spectrometer (formerly Varian, Inc.) at the room temperature (around 20 ^{o}C inside the bore). A presat pulse sequence was used to collect CEST spectra with a 5 s square-shape hard pre-saturation pulse at a power level of 25 db

(equivalent to B_1 = 9.4 μT) and the arrayed saturation frequency offset from +8,000 Hz to -8,000 Hz, and a step of -100 Hz (namely, 161 spectra in total were acquired in order to obtain a CEST spectrum).

For CEST dependence on concentration (Fig. 2d), a much shorter saturation duration time of 3 s was used. Other parameters were same as stated above.

9) MRI protocols

MRI CEST images were recorded with an Agilent Technologies 9.4 T / 31 cm bore-hole small animal MRI system (formerly Varian, Inc.) with a 38 mm quad coil (Doty Scientific, Inc.) as both excitation and receiver device. The temperature inside the magnet bore was around 20 ^{o}C. A customer modified fast spin echo (fsems) pulse sequence was used to acquire MRI raw images. The key modification was that a 3 s hard pre-saturation pulse at power level of 36 db (equivalent to B_1 = 8.2 μT) was applied at different saturation frequency offsets, varying from +10 ppm to -10 ppm with a decreased step of 0.2 ppm. Other major parameters are: the repetition time TR = 3.15 s, ETL = 8, ESP = 4, kzero = 4, the effective echo time TE_{eff} = 48 ms, 1 average, 2 dummy scans, the matrix size of 128x128, the field of view (FOV) = 30 x 30 mm and the slice thickness of 1 mm.

10) CEST spectral fitting method

The CEST spectra were fitted to a 2-pool or 3-pool chemical exchange model of Block Equations using the Matlab platform (version 7.0, Mathworks, Natick, MA) by following the published procedures.[3]

Tables S1. The parameters for fitting the CEST spectrum of PEG_{114}-*b*-$PDPA_{116}$ at pH 5.0 presented in **Fig. 2a** of the main text.[a)]

τ_{ex}**NH** (μs)	B_1 (Hz)	**Δδ** (ppm)	T_1**Water** (s)	T_2**Water** (s)	T_1**NH** (s)	T_2**NH** (s)
890	400	3.90	3.00	1.31	1.11	0.002

a) The parameters listed in this Table:

τ_{ex}NH: the lifetime of proton on the tertiary amines of block copolymer (in unit of micro-second)

B_1: the power of the pre-saturation pulse (in unit of Hz)

Δδ: the chemical shift difference between the proton of tertiary amines of block copolymer and the bulk water (in unit of ppm)

T_1 or T_2 values: the corresponding longitudinal or transversal relaxation times (in unit of second)

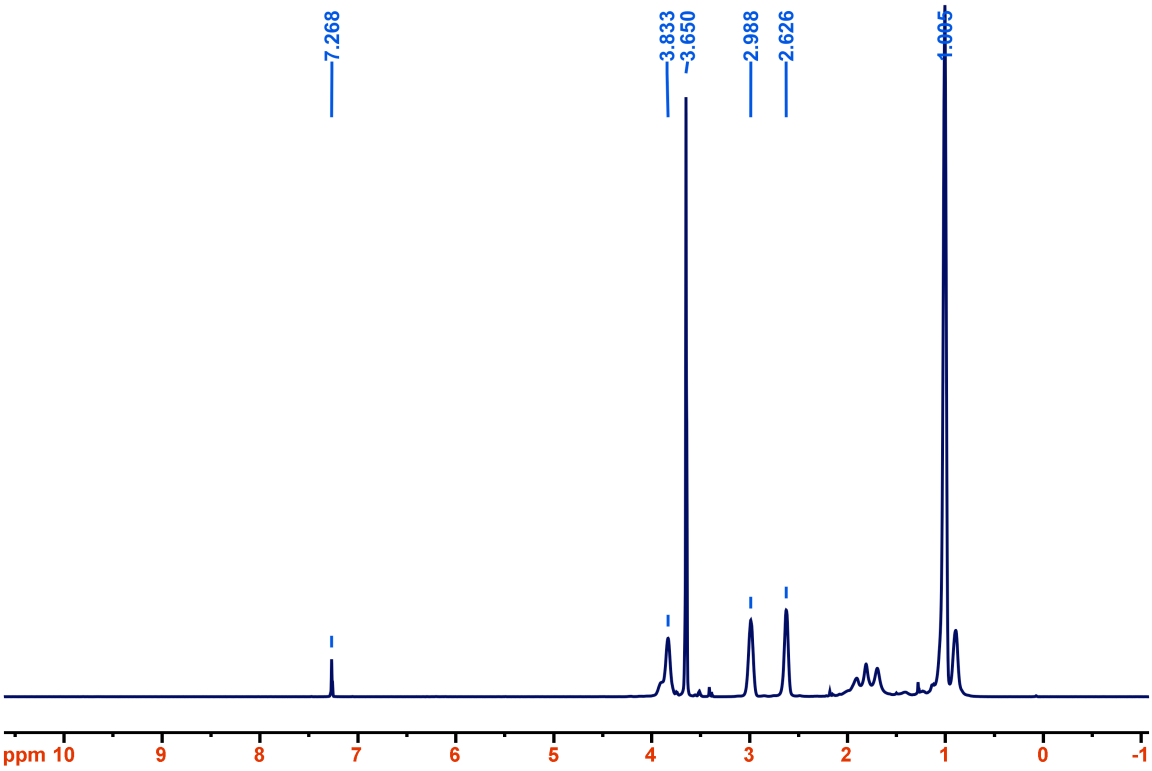

Figure S1. ^{1}H NMR spectrum of PEG_{114}-*b*-$PDPA_{116}$ in $CDCl_3$. The spectrum was recorded using a Varian 500 MHz NMR spectrometer.

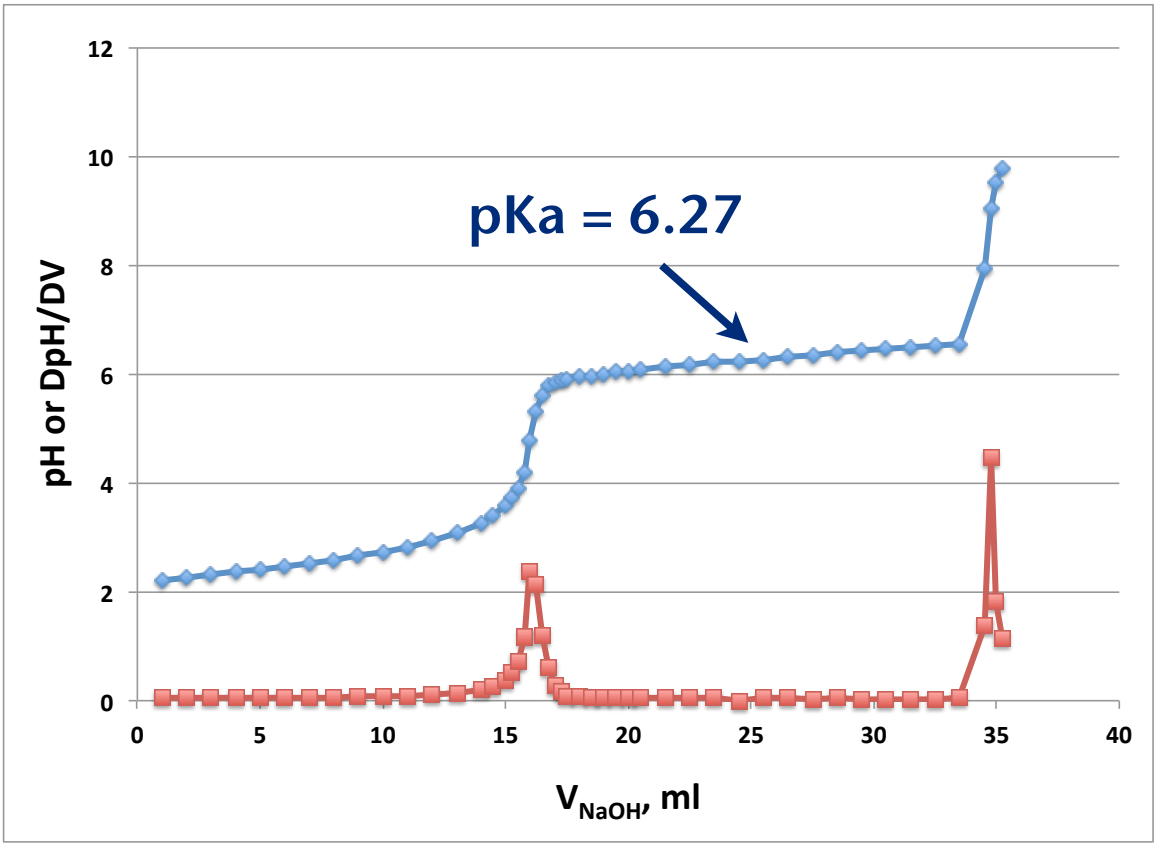

Figure S2. pH titration curve and the corresponding differential curve of 88 mg PEG_{114}-*b*-$PDPA_{116}$ with 0.02 M NaOH aqueous solution.

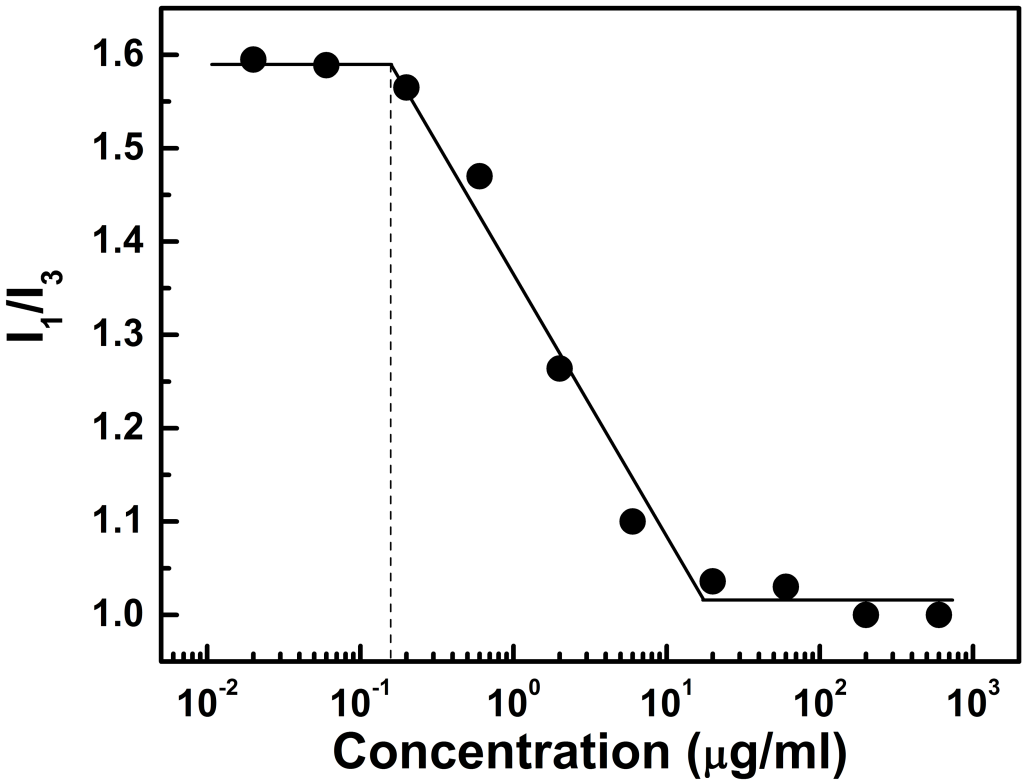

Figure S3. A plot of I_1/I_3 values *vs.* the concentrations for PEG_{114}-*b*-$PDPA_{116}$, which yielded a CMC of 0.15 μg/ml.

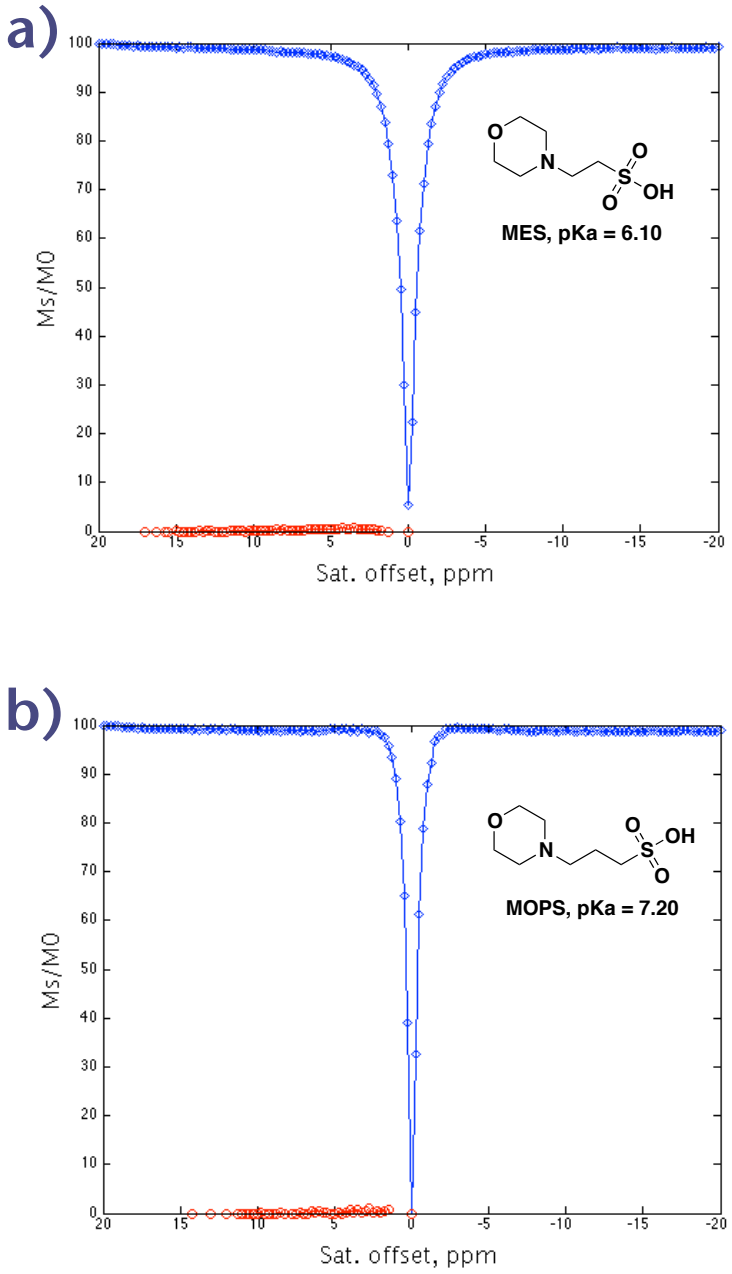

Figure S4. The CEST spectra of pure buffers: a) 0.1 M MES at pH 5.3 and b) 0.1 M MOPS at pH 7.5, respectively. The CEST asymmetries were also presented to better visualize the CEST effects (namely, $CEST_{asym} = [M_s/M_0]_{downfield} - [M_s/M_0]_{upfield}$).

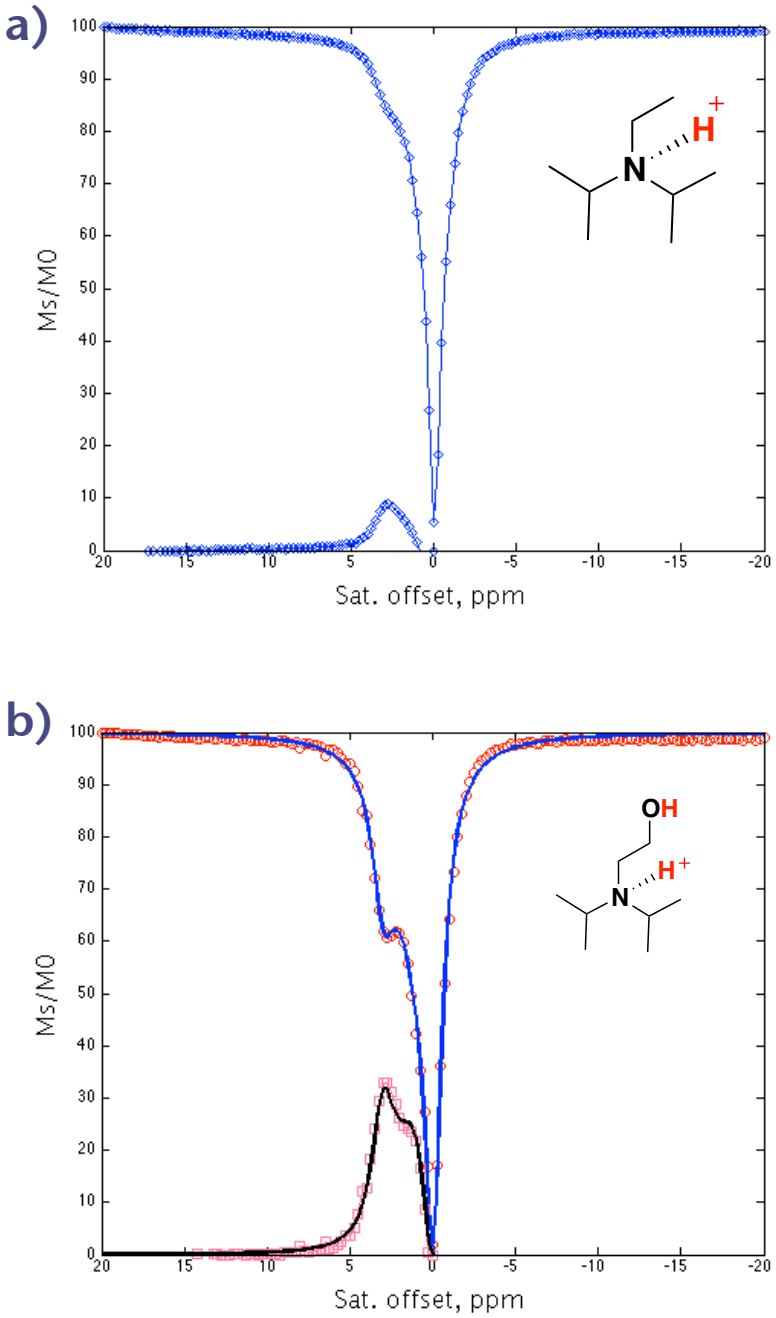

Figure S5. The CEST spectra of small analog molecules: a) 116 mM N,N-diisopropylethylamine (DIPEA) in 0.1 M MES at pH 5.3 and b) 116 mM *N*,*N*-diisopropylaminoethanol (DIPAE) in 0.1 M MOPS at pH 5.8, respectively. The CEST asymmetries were also presented to better visualize the CEST effects (namely, $CEST_{asym} = [M_s/M_0]_{\text{downfield}} - [M_s/M_0]_{\text{upfield}}$).

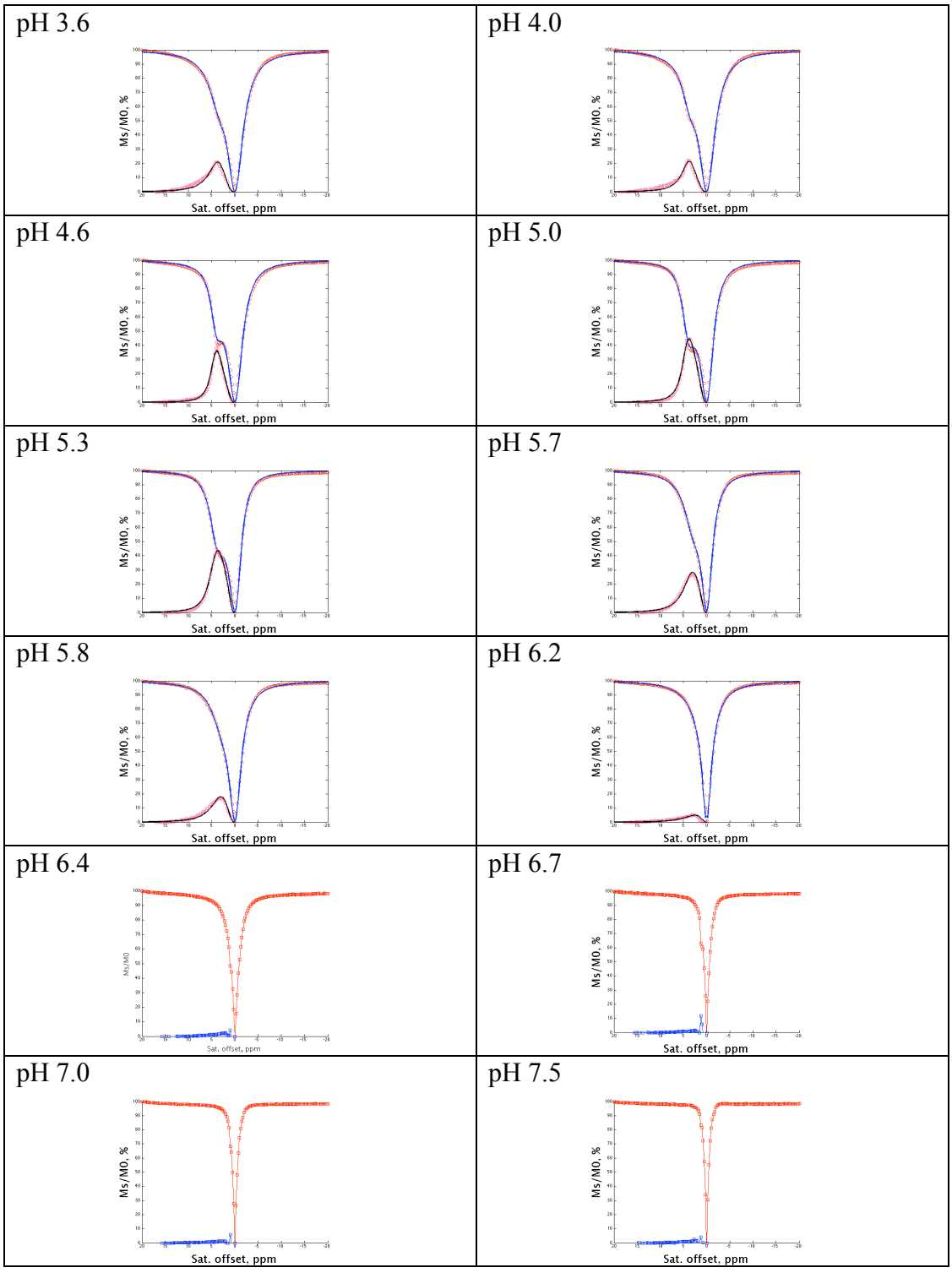

Figure S6. The CEST spectra of 0.5 mM PEG_{114}-*b*-$PDPA_{116}$ in 0.1 M MES and/or MOPS at the different pH values as labeled in the figures. The CEST asymmetries were also presented to better visualize the CEST effects (namely, $CEST_{asym} = [M_s/M_0]_{\text{downfield}} - [M_s/M_0]_{\text{upfield}}$).

11) References:

1. K. Zhou, Y. Wang, X. Huang, K. Luby-Phelps, B. D. Sumer and J. Gao, *Angewandte Chemie International Edition*, 2011, **50**, 6109-6114.
2. N. Nasongkla, E. Bey, J. Ren, H. Ai, C. Khemtong, J. S. Guthi, S.-F. Chin, A. D. Sherry, D. A. Boothman and J. Gao, *Nano Letters*, 2006, **6**, 2427-2430.
3. D. E. Woessner, S. Zhang, M. E. Merritt and A. D. Sherry, *Magnetic Resonance in Medicine*, 2005, **53**, 790-799.